Supporting Information

Targeted Photothermal Release of Antibiotics by a Graphene Nanoribbon-Based Supramolecular Glycomaterial

Ying Shang,[1‡] Sheng Zhang,[1‡] Hui-Qi Gan,[1‡] Kai-Cheng Yan,[1,5] Fugui Xu,[2] Yiyong Mai,[2] Daijie Chen,[3] Xi-Le Hu,[1]* Lei Zou,[1]* Tony D. James[5,6]* and Xiao-Peng He[1,4]*

[1]*Key Laboratory for Advanced Materials and Joint International Research Laboratory of Precision Chemistry and Molecular Engineering, Feringa Nobel Prize Scientist Joint Research Center, School of Chemistry and Molecular Engineering, East China University of Science and Technology, 130 Meilong Rd., Shanghai 200237, China*
[2]*School of Chemistry and Chemical Engineering, Frontiers Science Center for Transformative Molecules, Shanghai Key Laboratory of Electrical Insulation and Thermal Ageing, Shanghai Jiao Tong University, 800 Dongchuan RD. Minhang District, Shanghai 200240, China*
[3]*School of Pharmacy, Shanghai Jiao Tong University, 800 Dongchuan RD. Minhang District, Shanghai 200240, China*
[4]*National Center for Liver Cancer, the International Cooperation Laboratory on Signal Transduction, Eastern Hepatobiliary Surgery Hospital, Shanghai 200438, China*
[5]*Department of Chemistry, University of Bath, Bath, BA2 7AY, UK*
[6]*School of Chemistry and Chemical Engineering, Henan Normal University, Xinxiang 453007, China*
[‡]*Equal contribution*

Corresponding authors. xphe@ecust.edu.cn (X.-P. He), chstdj@bath.ac.uk (T. D. James), zoulei@ecust.edu.cn (L. Zou), xlhu@ecust.edu.cn (X.-L. Hu)

Contents list

1 Experimental Section

All purchased chemicals and reagents were of analytical grade. *Pseudomonas aeruginosa* (*P. aeruginosa*, ATCC 27853) was obtained from ATCC (American Type Culture Collection, Beijing Zhongyuan Ltd). Absorption spectra were measured on a Varian Cary 500 UV−vis spectrophotometer. Fluorescence spectra were obtained on a Varian Cary Eclipse fluorescence spectrophotometer. Zeta potentials were determined on a Horiba LB- 550 dynamic light scattering nano-analyzer. Fluorescence imaging was carried out using a Nikon AIR confocal laser-scanning microscope.

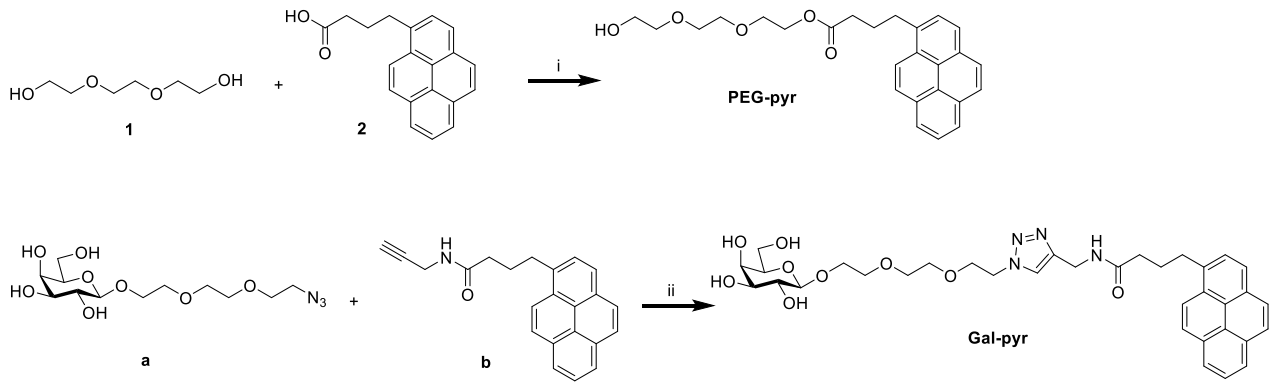

Scheme S1. Synthesis of **PEG-pyr** and **Gal-pyr**. Reagents and conditions: (i) 1,3-dicyclohexylcarbodiimide (DDC) in MeCN; (ii) $CuSO_4 \cdot H_2O$, sodium ascorbate in THF/H_2O.

Synthesis of PEG-pyr. To a solution of **2** (177 mg, 0.6 mmol) in CH_3CN (10 mL), DCC (253 mg, 1.2 mmol) was added, and the resulting mixture was stirred at room temperature for 3 h. Then, **1** (42.6 mg, 0.61 mmol) was added, and the resulting mixture was stirred at room temperature for 6 h under an argon atmosphere. Then, the mixture was diluted by CH_2Cl_2 and washed by brine. The combined organic layer was dried over $MgSO_4$, filtered, and concentrated in vacuum to give a crude product, which was purified by column chromatography (CH_2Cl_2/MeOH = 10:1, v/v) to obtain **PEG-pyr** as a yellow solid (21 mg, 86%). TLC: R_f 0.2 (CH_2Cl_2/MeOH = 10:1, v/v). ^{1}H NMR (400 MHz, $CDCl_3$): δ 8.29 (d, J = 8.4 Hz, 1H), 8.16–8.15 (m, 2H), 8.11–8.08 (m, 2H), 8.02–7.95 (m, 3H), 7.85–7.83 (d, J = 7.6 Hz, 1H), 4.26–4.23 (t, J = 6.8 Hz, 2H), 3.68–3.65 (m, 4H), 3.60 (s, 4H), 3.54–3.52 (t, J = 5.9 Hz, 2H), 3.39–3.35 (t, J = 6.3 Hz, 2H), 2.51–2.47 (t, J = 5.9 Hz, 2H), 2.22–2.15 (m, 3H); ^{13}C NMR (101 MHz, $CDCl_3$): δ 170.4, 146.2, 131.7, 129.7, 129.6, 125.8, 122.6, 120.7, 120.5, 120.3, 86.2, 73.9, 70.9, 70.8, 67.9, 66.9, 64.1, 61.2, 20.5. HRMS (ESI, *m/z*): $[M + K]^+$ calcd for $C_{26}H_{28}O_5K^+$ 459.1574, found 459.2356.

Synthesis of Gal-pyr. To a solution of **a** (281.4 mg, 0.6 mmol)[1] and **b** (200 mg, 0.6 mmol)[2] in THF/H_2O (10 mL/2 mL, v/v), sodium ascorbate (443 mg, 2.2 mmol) and $CuSO_4 \cdot 5H_2O$ (280 mg, 1.1 mmol) were added. The resulting mixture was stirred at room temperature for 12 h under an argon atmosphere. Then, the mixture was diluted by CH_2Cl_2 and washed using EDTA (5 mL, 300 mmol) and

then brine. The combined organic layer was dried over $MgSO_4$, filtered, and concentrated in vacuum to give a crude product, which was purified by column chromatography (CH_2Cl_2/MeOH = 5:1, v/v) to obtain **Gal-pyr** as a yellow solid (25 mg, 82%). TLC: R_f 0.3 (CH_2Cl_2/MeOH = 5:1, v/v). ^{1}H NMR (400 MHz, Methanol-d_4): δ 8.29 (d, J = 9.3 Hz, 1H), 8.21–8.08 (m, 4H), 8.03 (s, 2H), 7.99 (t, J = 7.6 Hz, 1H), 7.94–7.83 (m, 2H), 4.64–4.60 (m, 1H), 4.51 (t, J = 4.9 Hz, 2H), 4.47 (s, 1H), 4.15 (d, J = 7.5 Hz, 1H), 3.88–3.81 (m, 1H), 3.79–3.76 (m, 3H), 3.76–3.66 (m, 2H), 3.57–3.45 (m, 3H), 3.45–3.42 (m, 7H), 3.38–3.32 (m, 2H), 2.40 (t, J = 7.3 Hz, 2H), 2.23–2.08 (m, 2H); ^{13}C NMR (101 MHz, Methanol-d_4): δ 175.6, 137.2, 132.6, 132.1, 131.2, 129.7, 128.4, 128.2, 127.5, 126.8, 126.0, 125.9, 125.8, 125.6, 124.9, 124.3, 104.8, 76.5, 74.7, 72.3, 71.1, 70.1, 69.3, 62.3, 51.2, 36.4, 35.4, 33.6, 28.9. HRMS (ESI, *m/z*): $[M + Na]^+$ calcd for $C_{35}H_{42}N_4O_9Na^+$ 685.2849, found 685.2848.

High-resolution transmission electron microscopic (HRTEM) and zeta potential measurement. GNR-PEO (7.5 μg mL^{-1}) or **PEG-pyr/Gal-pyr/GNR-PEO** (3 μM/7 μM/7.5 μg mL^{-1}) was dropped onto 200 mesh holey carbon copper grid, and then dried under atmospheric pressure. Then, HRTEM images were recorded on JEOL 2100 equipped with a Gatan Orius charged-coupled device camera (Tridiem energy filter operating at 200 kV) and Talos F200X TEM. A Malvern Zetasizer Nano ZS instrument was used to measure zeta potential. A deionized water solution of **GNR-PEO** (7.5 μg mL^{-1}) or **PEG-pyr/Gal-pyr/GNR-PEO** (3 μM/7 μM/7.5 μg mL^{-1}) was moved into a pre-rinsed folded capillary cell, and measurements were done at 25 °C for all samples using an applied voltage of 150 V. A minimum of three replicates were done for each sample.

Synthesis of GNR-PEO2000. GNR-PEO2000 was prepared following our previously reported protocol. Briefly, **GNR-COOH** (50 mg, 0.03 mmol repeating units) and poly (ethylene oxide) (**PEO**, 0.6 mmol) were added into a dried 100 mL Schlenk tube. Then, a mixed solvent of dry THF (30 mL) and DMF (15 mL) was added into the tube. Strong sonication was applied to obtain a homogeneous dispersion. Then, dimethylaminopyridine (DMAP, 2.2 mg, 4.6 × 10^{-3} mmol) was added into the mixture, which was further stirred for several minutes. After the mixture was cooled to 0 ℃, 1-(3-dimethylaminopropyl)-3-ethylcarbodiimide hydrochloride (EDC, 27.5 mg, 0.037 mmol) was added. The mixture was stirred at 0 ℃ for 30 min and then at room temperature for 3 days. Afterwards, the mixture was dialyzed with a membrane of 14 kDa molecular weight cutoff against pure water by renewing the external water for more than 10 times over a period of 3 days to remove the unreacted PEO. Finally, the resulting mixture was freeze-dried for 2 days to yield **GNR-PEO2000**.[3]

Preparation of PEG-pyr/Gal-pyr/GNR-PEO. To a deionized water solution of **GNR-PEO** (1 mL, 15 μg mL^{-1}), **PEG-pyr/Gal-pyr** with varying molar ratios (10 μL, 2 mM) was added. The resulting mixture was sonicated for 10 min, and then stirred at room temperature for 12 h in the dark. The mixture

was then centrifuged three times at 10000 rpm for 20 min to remove residual compounds to obtain the supramolecular glycomaterial.

Preparation of TMP/PEG-pyr/Gal-pyr/GNR-PEO Composites. A deionized water (50 mL) solution of **PEG-pyr/Gal-pyr/GNR-PEO** (0-20 μM/20-0 μM/15 μg mL^{-1}) was sonicated for 30 min. Then, 100 μL DMSO solution of trimethoprim (**TMP**) (0.5 g mL^{-1}) was added for a further sonication for 30 min. Free **TMP** molecules were excluded by centrifugation at 10000 rpm for 20 min to obtain the **PEG-pyr/Gal-pyr/GNR-PEO/TMP** composite. To calculate the **TMP** loading efficiency, the absorbance of the supernatant was measured at 280 nm using a Varian Cary 500 UV−vis spectrophotometer and compared to a standard curve. The loading efficiency was calculated by subtracting the unloaded **TMP** from added **TMP**.[4,5] Loading of other antibiotics followed the same procedures.

Quantification of Gal-pyr by the anthrone method. To prepare the anthrone reagent, 100 mg of anthrone was dissolved in 50 mL of concentrated H_2SO_4 (95%). To a 1 mL deionized water solution of different supramolecular glycomaterials (**PEG-pyr/Gal-pyr**/**GNR-PEO** containing **PEG-pyr**/**Gal-pyr** at varying molar ratios), 3 mL of the anthrone reagent was added, and the mixture was vortexed and then incubated at 90 ℃ for 15 minutes. After the mixture was cooled down to temperature, the UV−vis absorption at 627 nm was detected by a Varian Cary 500 UV−vis spectrophotometer. **Gal-pyr** was quantified by comparing to a standard curve based on D-galactose.[6]

Bacterial cultures and viability tests. *P. aeruginosa* (ATCC 27853) cells was cultured in a Luria-Bertani (LB) culture medium (20 mL), which were allowed to grow at 37 °C with shaking for 12 h. The plate-counting method was used to determine the number of colony-forming units (CFU). *P. aeruginosa* cells were seeded at a density of 10^6 CFU mL^{-1} in a 96-well plate, followed by incubation with antibiotics or different glycomaterials in the absence and presence of light irradiation (808 nm, 1 W cm^{-2}, 15 min). The resulting suspensions were cultured for 3 h, diluted, and then spread on agar culture plate by the spread plate method. Following another incubation at 37 °C for 16–20 h, bacterial CFUs were counted and the corresponding viabilities were calculated using the following formula (eq 1). All experiments were run in triplet.

$$\text{Viability}\% = \left(\frac{C1}{C}\right) \times 100\% \quad (1)$$

where C1 and C are the bacterial CFUs of the experimental (treated with different antibiotics and glycomaterials) and control group (treated with sterile water), respectively.

Eradication of *Pseudomonas aeruginosa*-derived biofilms. *P. aeruginosa* (ATCC 27853) from a single colony was cultured in a LB medium (2 mL). Then, the culture was placed in an orbital shaker (180 r. p. m.) for 16 h at 37 °C. The resulting culture was diluted with fresh LB medium to an OD_{600} of 0.02, and then was transferred to a 96-well microtiter plate. Then, cultures were incubated for 16 h at 37 °C to obtain the *P. aeruginosa*-based biofilms.[7] To evaluate antibacterial activity, the established *P. aeruginosa* biofilms were coated on glass slides, followed by addition of different materials. Then, the glass slides were irradiated with 808 nm laser light (1 W cm^{-2}) for 30 min, and then incubated for 16 h at 37 °C. Subsequently, 20 μL of live/dead staining solution (Syto9/propidium iodide (PI)) was added onto the glass slices with a final concentration of Syto9 and PI being 1.4 μM and 8.3 μM, respectively. Finally, the glass slides were placed inside a well plate covered with a fresh air-permeable foil, and then moved to an incubator for 2 h at 37 °C prior to fluorescence imaging. The different proportions of green (Syto9: live bacteria) and red (PI: dead bacteria) biovolumes were calculated using ImageJ software.

2 Additional Figures

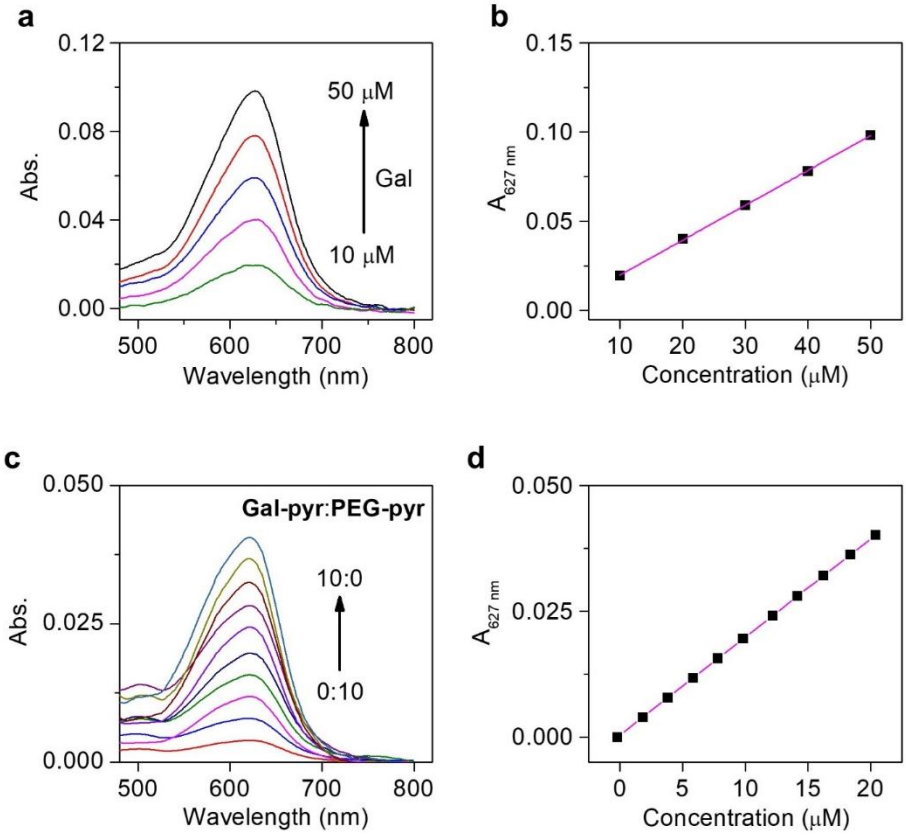

Figure S1. (a) UV-vis absorption spectra of glycoaldehyde converted from D-galactose (Gal) in the presence of anthrone and H_2SO_4. (b) Plotting the maximum UV-vis absorption intensity of glycoaldehyde as a function of Gal concentration. (c) UV-vis absorption spectra of glycoaldehyde converted from **Gal-Pyr** on the supramolecular glycomaterials (**PEG-pyr**/**Gal-pyr**/**GNR-PEO**) containing **PEG-pyr**/**Gal-pyr** at varying molar ratios in the presence of anthrone and H_2SO_4. (d) Plotting the UV-vis maximum absorption intensity of glycoaldehyde as a function of **Gal-pyr** concentration.

According to equation (1), the concentrations of **Gal-pyr** from supramolecular glycomaterials containing **PEG-pyr**/**Gal-pyr** with varying molar ratios (From 10:0 to 0:10) were calculated to be ~0, 1.8 μM, 3.8 μM, 5.8 μM, 7.8 μM, 9.8 μM, 12.2 μM, 14.2 μM, 16.2 μM, 18.4 μM and 20.4 μM, respectively.

$$X = \frac{(Y - 3.7\times10^{-4})}{0.00195} \quad (1)$$

where Y is the absorption of anthrone at 627 nm.

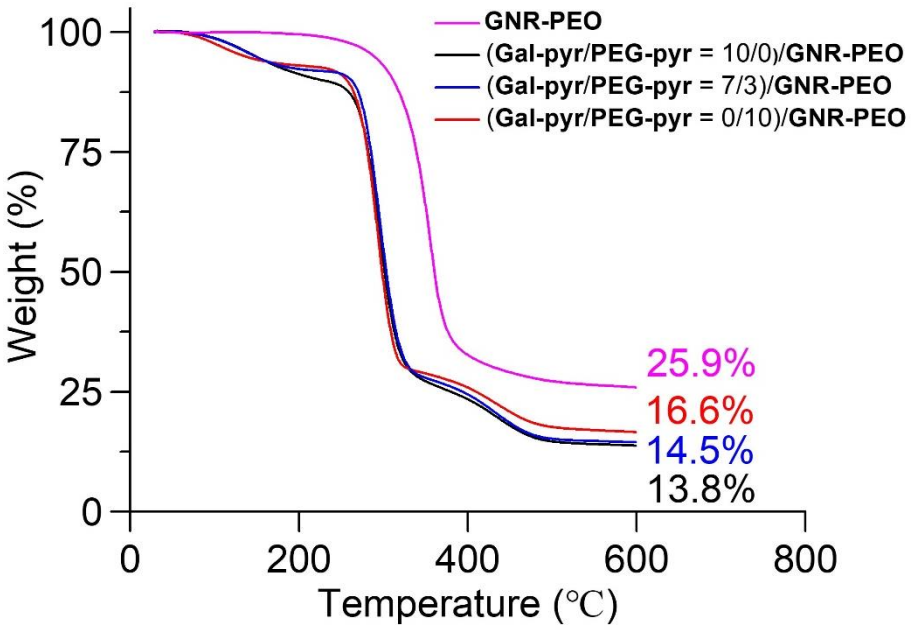

Figure S2. TGA curves of **GNR-PEO**, (**Gal-pyr**:**PEG-pyr** = 10:0)/**GNR-PEO**, (**Gal-pyr**:**PEG-pyr** = 7:3)/**GNR-PEO** and (**Gal-pyr**: **PEG-pyr** = 0:10)/**GNR-PEO** measured under N_2 atmosphere (40 mL min^{-1}) with an increasing temperature rate of 10 °C min^{-1}. The weight percentage of the GNR backbone is determined to be 25.9%.

The total weight of **Gal-pyr/PEG-pyr** on the glycomaterials were then determined by equation (2). We note that TGA requires a large amount of samples; therefore we only used three representative samples (**Gal-pyr/PEG-pyr** = 10:0, 3:7 and 0:10) for the analysis.

$$\boldsymbol{M}_{\mathbf{PEG-pyr}} + \boldsymbol{M}_{\mathbf{Gal-pyr}} = \boldsymbol{M}_{\mathrm{t}} \times (1 - \boldsymbol{W}_{\mathrm{residue}}) - 1.21 \qquad (2)$$

where W_{residue} is the weight percentage of the **GNR-PEO** backbone after thermal treatment over 500 °C according to the TGA curve, 1.21 is the weight of the grafted PEO chains on **GNR-PEO** expressed in mg, M_{t} is the total weight of a TGA sample, and $M_{\mathbf{PEO\text{-}pyr}}$ and $M_{\mathbf{Gal\text{-}pyr}}$ are the weight of PEO-pyr and **Gal-pyr**, respectively; the weight of **Gal-pyr** was obtained from the anthrone method.

According to both equations (1) and (2), the concentrations of **Gal-pyr** and **PEG-pyr** in the groups of (**Gal-pyr**:**PEG-pyr** = 10:0)/**GNR-PEO**, (**Gal-pyr**:**PEG-pyr** = 7:3)/**GNR-PEO** and (**Gal-pyr**:**PEG-pyr** = 0:10)/**GNR-PEO** were determined to be 20.4 μM/0.3 μM, 14.2 μM/5.9 μM and ~0/18.8 μM. The calculated ratios are close to the ratios of the final added concentrations between **PEG-pyr** and **Gal-pyr**.

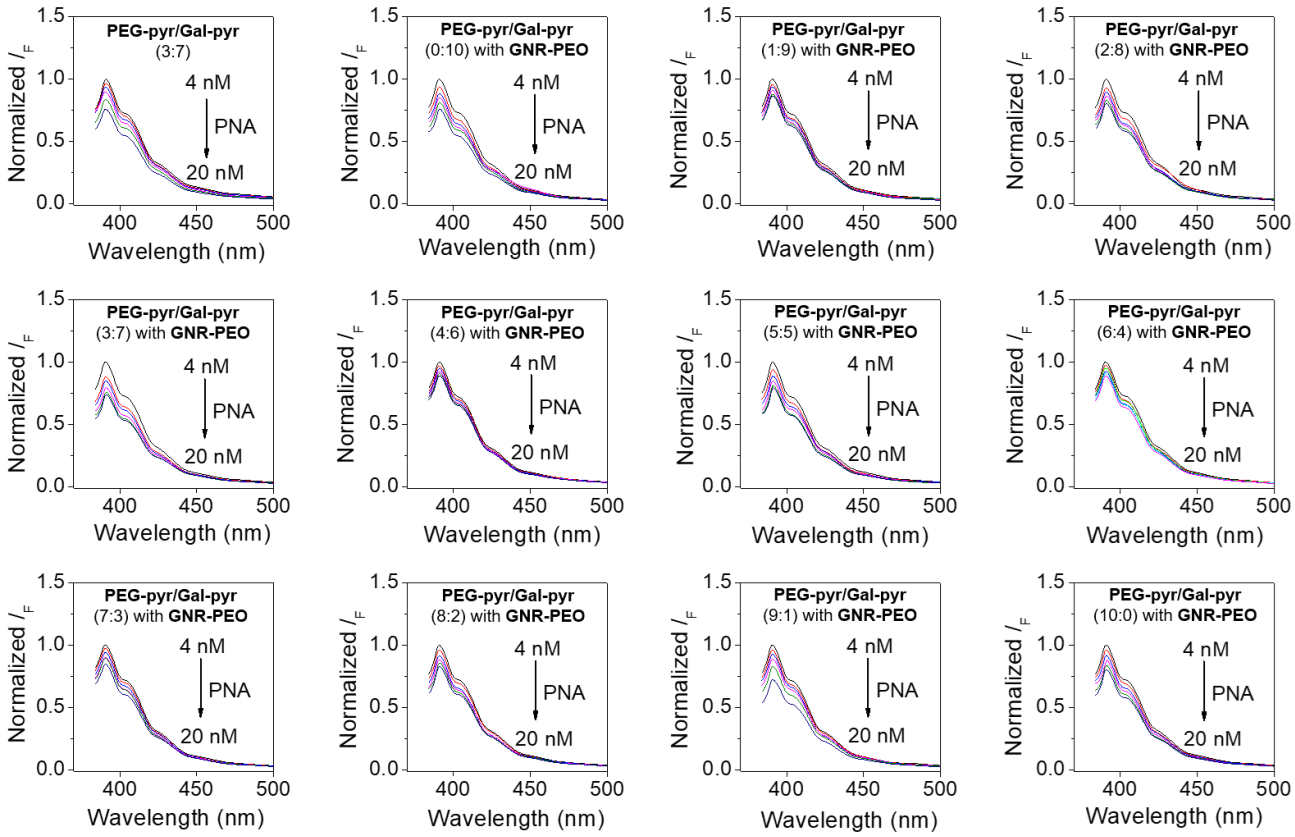

Figure S3. Fluorescence emission spectra of **PEG-pyr/Gal-pyr** at varying molar ratios (fixed concentration = 20 μM) with increasing concentrations of PNA (4-20 nM) in the absence and presence of **GNR-PEO** (15 μg mL^{-1}) in deionized water. Excitation wavelength = 370 nm.

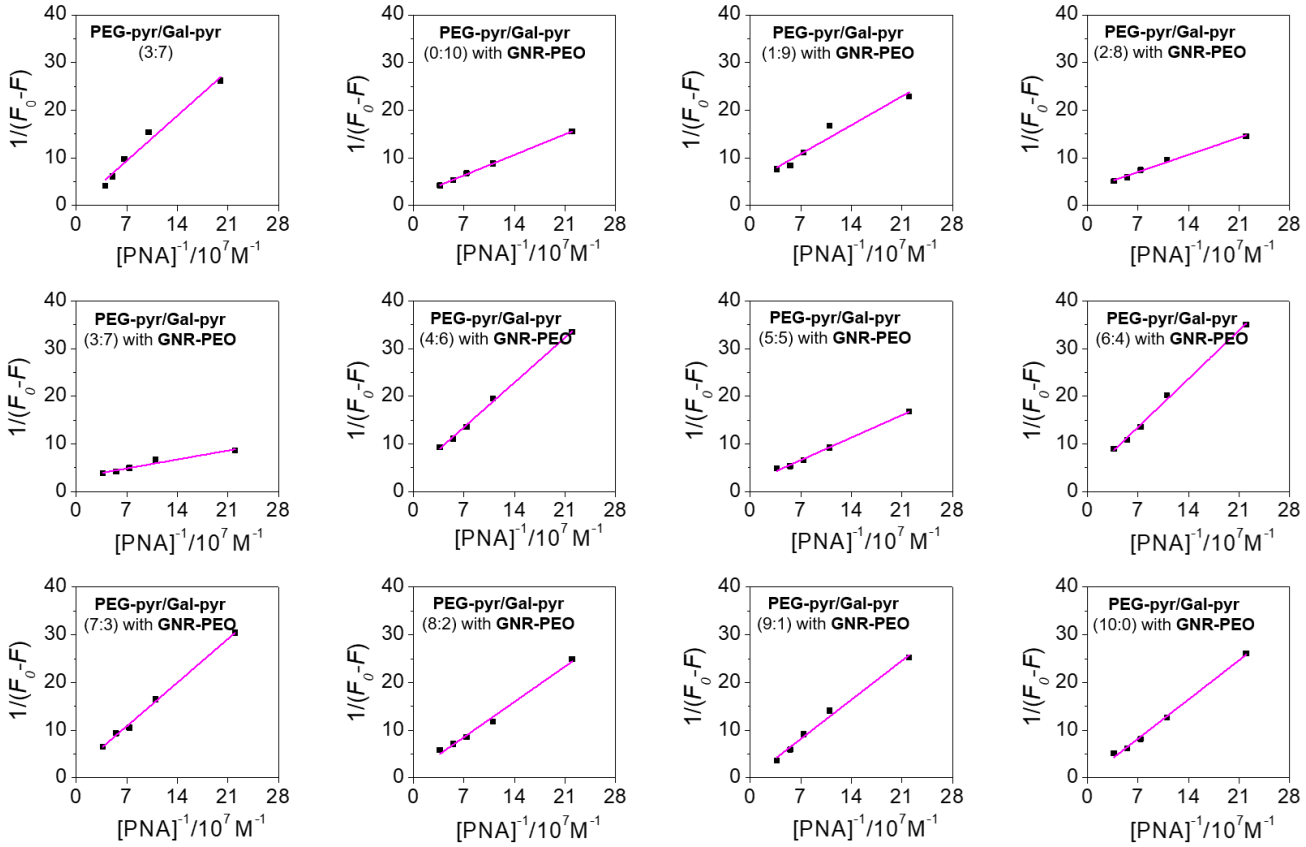

Figure S4. Measuring the binding constants (K_a) between the supramolecular glycomaterials with **PEG-pyr/Gal-pyr** at different ratios (fixed concentration = 20 μM) in the absence and presence of **GNR-PEO** (15 μg mL^{-1}) with PNA in deionized water. K_a values were calculated by the following equation (eq 2).

$$(F_0 - F)^{-1} = {F_0}^{-1} + (K_a F_0 C_{PNA})^{-1} \quad (2)$$

where F_0 and F are the fluorescence intensity of supramolecular glycomaterials without and with increasing concentrations of PNA, respectively; C_{PNA} is the concentration of PNA; K_a represents the binding constant.[8,9]

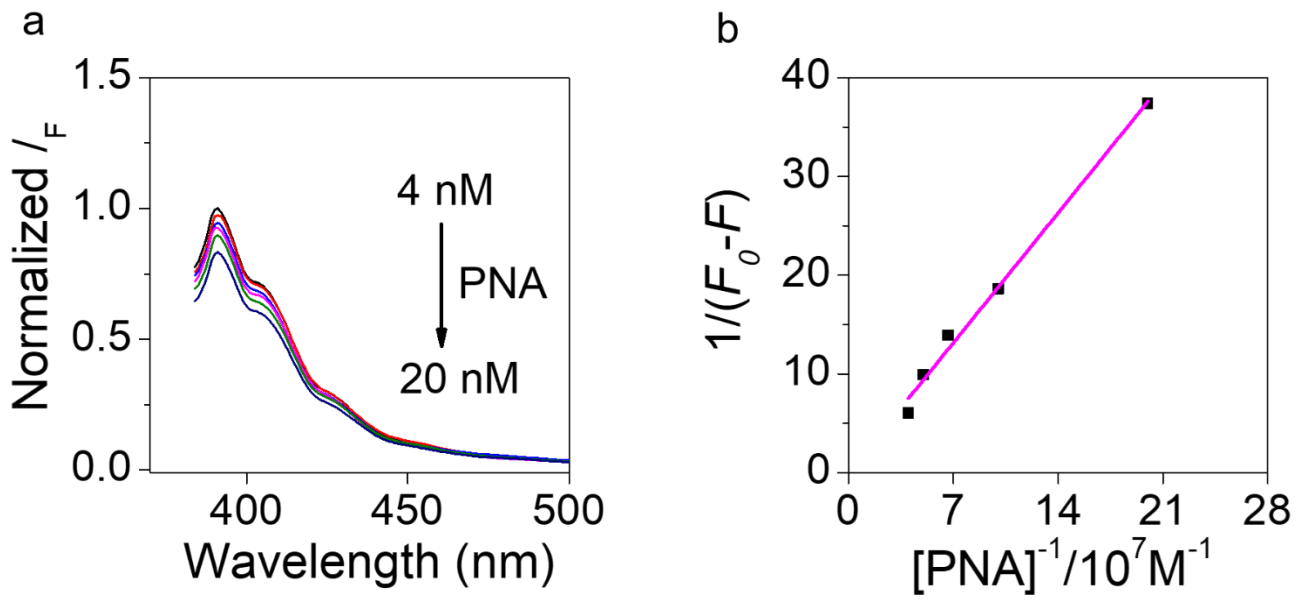

Figure S5. (a) Fluorescence emission spectra of **PEG-pyr/Gal-pyr/GNR-PEO** (6 μM/14 μM/15 μg mL^{-1}) with increasing concentrations of PNA (4-20 nM) pre-treated with an excess of free β-D-galactose (10 mM) in deionized water. Excitation wavelength = 370 nm. (b) Measuring the binding constants (K_a) between **PEG-pyr/Gal-pyr/GNR-PEO** (6 μM/14 μM/15 μg mL^{-1}) and PNA pre-treated with an excess of free β-D-galactose (10 mM) in deionized water.

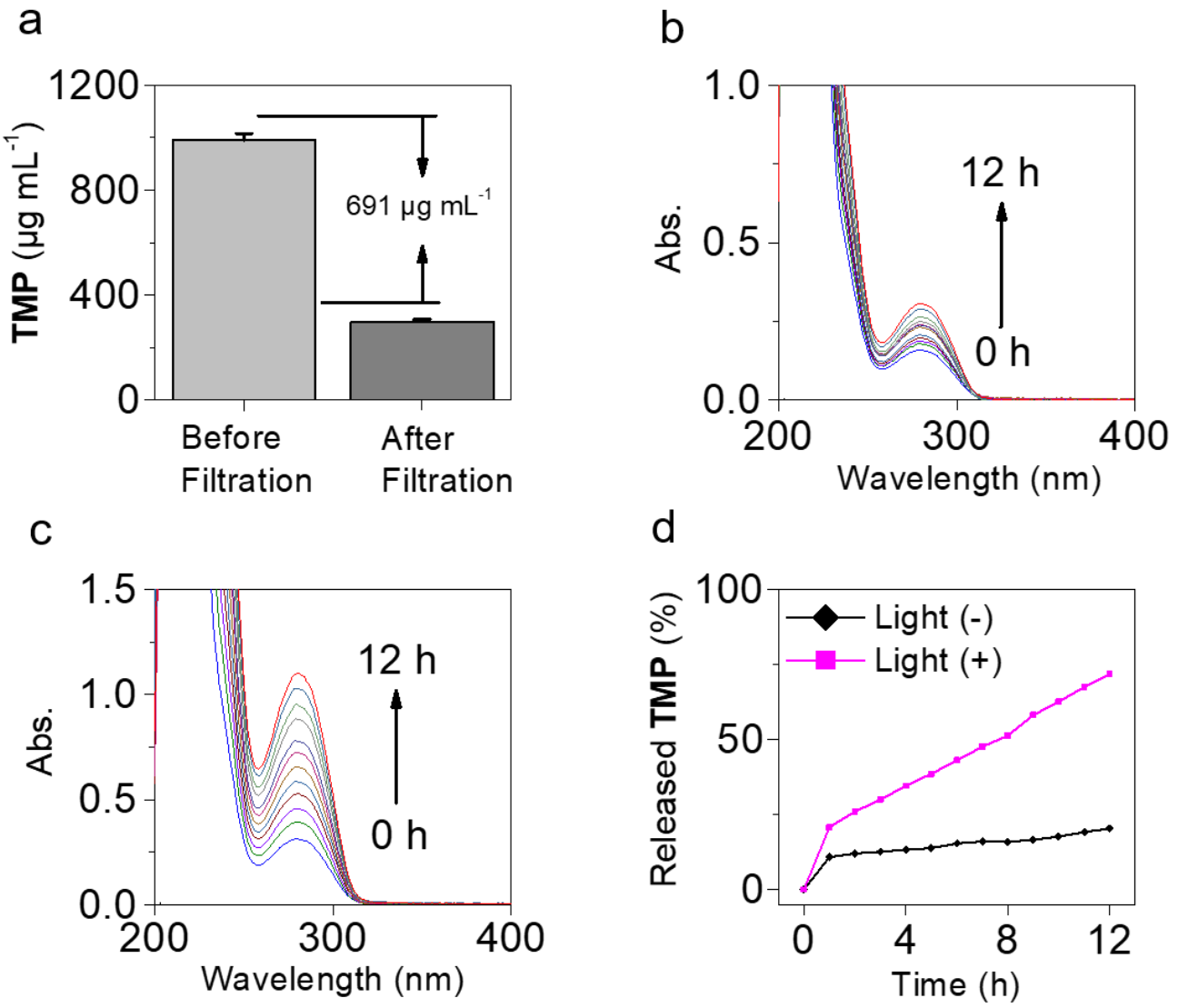

Figure S6. (a) Quantification of the **TMP**-loading capacity of **PEG-pyr/Gal-pyr/GNR-PEO** (6 μM/14 μM/15 μg mL^{-1}). Time-dependent UV-vis absorption spectra of free **TMP** in the supernatant of **TMP**-loaded **PEG-pyr/Gal-pyr/GNR-PEO** after centrifugation (10000 rpm, 5 min) without (b) and with (c) light irradiation (808 nm, 1 W cm^{-2}, 0-12 h). (d) Time-dependent release of **TMP** from **PEG-pyr/Gal-pyr/GNR-PEO** (6 μM/14 μM/15 μg mL^{-1}) in Tris-HCl solution (0.01 M, pH 7.4) without and with light irradiation (808 nm, 1 W cm^{-2}, 0-12 h).

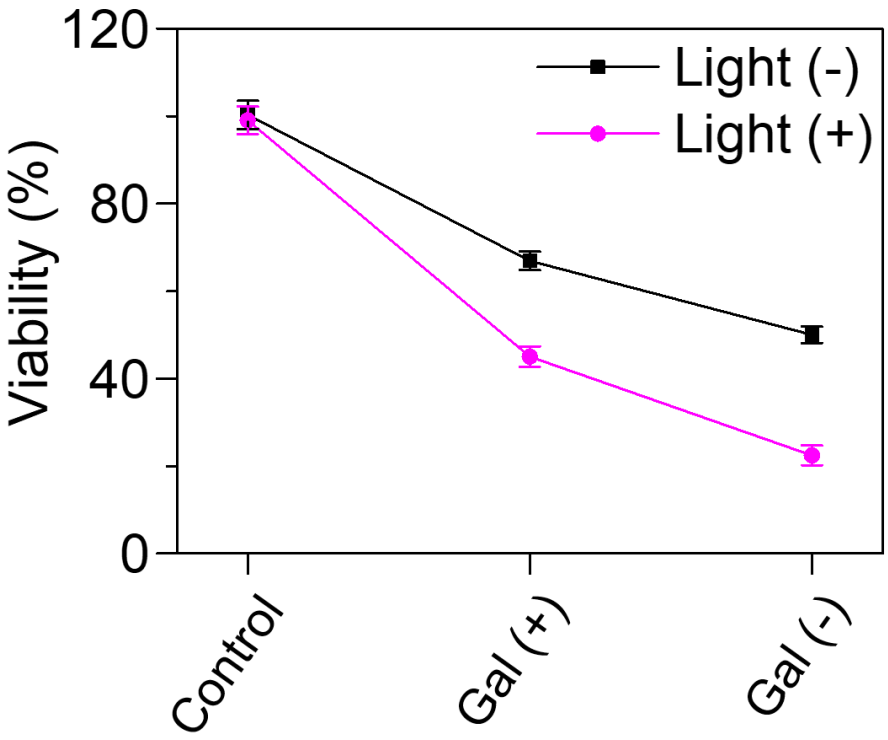

Figure S7. Relative viability of *P. aeruginosa* treated with **PEG-pyr/Gal-pyr/GNR-PEO** (6 μM/14 μM/15 μg mL^{-1}) without and with pretreatment of an excess of free β-D-galactose (10 mM) in the absence and presence of light irradiation (808 nm, 1 W cm^{-2}, 15 min).

Table S1. Binding constant (K_a) of the supramolecular glycomaterial with varying PEG-pyr/Gal-pyr ratios (0:10-10:0) for PNA measured in deionized water.

	K_a (10^7 M^{-1})	
	PEG-pyr/Gal-pyr ratio[a]	PNA[b]
w/ **GNR-PEO**[c]	0/10	3.3
	1/9	5.6
	2/8	6.7
	3/7	11.2
	4/6	3.1
	5/5	2.8
	6/4	2.3
	7/3	1.3
	8/2	1.1
	9/1	0.003
	10/0	0.00005
w/o **GNR-PEO**[d]	3/7	0.005
	0/10	0.009

[a]Molar ratio between **PEG-pyr** and **Gal-pyr** (fixed concentration: 20 μM); [b]Peanut agglutinin; [c]with **GNR-PEO**; [d]without **GNR-PEO**.

Table S2. Summary of the binding strength between PNA and various reported glycoclusters.

Lectin	Glycoclusters/glycomaterials	K_a	Ref
PNA	Lactose-modified triazatruxene glycocluster	$5.8 \times 10^5\ M^{-1}$	10
	Bivalent lactoside	$5.1 \times 10^4\ M^{-1}$	11
	Tetravalent lactoside	$3.5 \times 10^3\ M^{-1}$	
	Galactose	$1.7 \times 10^3\ M^{-1}$	
	Bivalent lactoside	$1.9 \times 10^3\ M^{-1}$	
	Thiodigalactoside	$1.5 \times 10^3\ M^{-1}$	12
	Thiodisaccharide	$1.3 \times 10^3\ M^{-1}$	
	Monovalent thiodigalactoside	$2.2 \times 10^3\ M^{-1}$	
	Divalent thiodigalactoside	$6.4 \times 10^3\ M^{-1}$	
	Tetravalent thiodigalactoside	$13.1 \times 10^3\ M^{-1}$	
	Monovalent α-D-galactose polymers	$6.3 \times 10^4\ M^{-1}$	13,14
	Monovalent β-D-galactose polymers	$2.5 \times 10^4\ M^{-1}$	
	Monovalent α-D- galactopyranoside	$1.8 \times 10^3\ M^{-1}$	
	Monovalent β-D- galactopyranoside	$1.0 \times 10^3\ M^{-1}$	
	Monovalent Lactose	$1.3 \times 10^3\ M^{-1}$	
	Lactose-based glycodendrimer	$6.2 \times 10^7\ M^{-1}$	15
	Glycocluster	$3.4 \times 10^5\ M^{-1}$	16
	Glycocluster	$1.8 \times 10^4\ M^{-1}$	17
	Monovalent α-D-galactoside	$1.8 \times 10^3\ M^{-1}$	18
	Monovalent β-D-galactoside	$0.9 \times 10^3\ M^{-1}$	
	Monovalent β-D-lactoside	$1.4 \times 10^3\ M^{-1}$	19
	Multivalent lactose-nucleo-cages	$10^5\ M^{-1}$	20
	Heptavalent glycodendrimer	$2.8 \times 10^5\ M^{-1}$	21
	Tetradecavalent glycodendrimer	$0.7 \times 10^5\ M^{-1}$	
	Heptakis-galactose β-cyclodextrin	$0.9 \times 10^5\ M^{-1}$	
Lectin	**Glycoclusters/glycomaterials**	**K_d**	**Ref**
PNA	Glycocluster	0.16 mM	22
	Glycocluster	34.8 nM	23
	Glycodendriprotein, mono-antennary-β-D-galactose	1.8×10^{-3} M	24
	Glycodendriprotein, bi-antennary-β-D-galactose	1.1×10^{-3} M	
	Glycodendriprotein, bi-antennary-β-D-galactose	1.5×10^{-3} M	
	Glycodendriprotein, tri-antennary-β-D-galactose	3.4×10^{-4} M	
	Glycodendriprotein, tetra-antennary-β-D-galactose	1.4×10^{-7} M	

3 Original spectra of new compounds

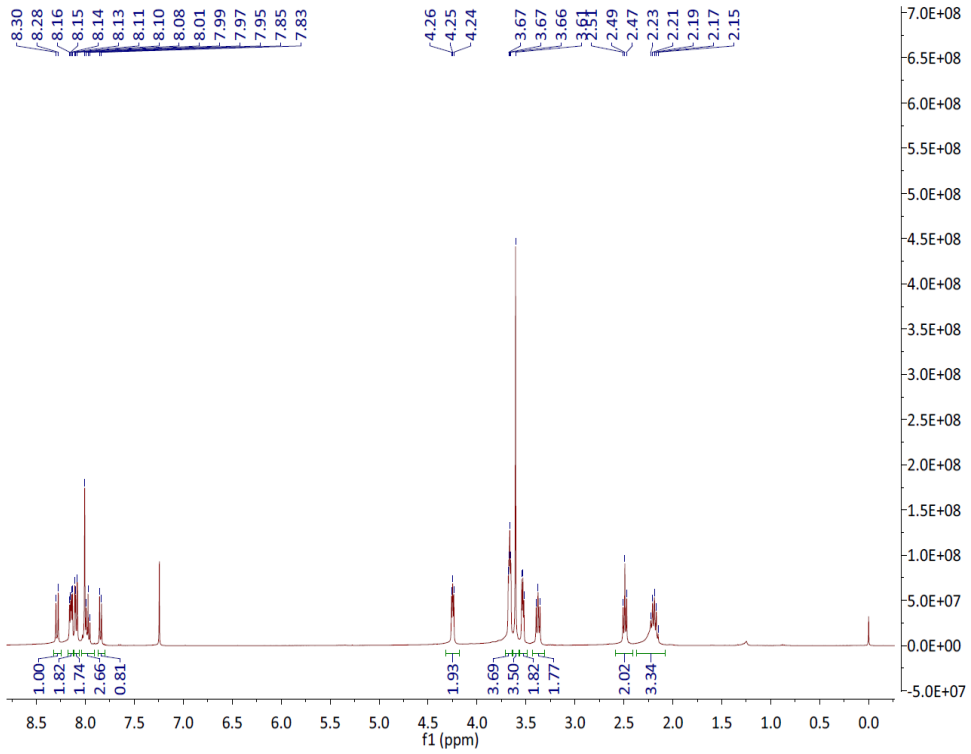

^{1}H NMR of **PEG-pyr**.

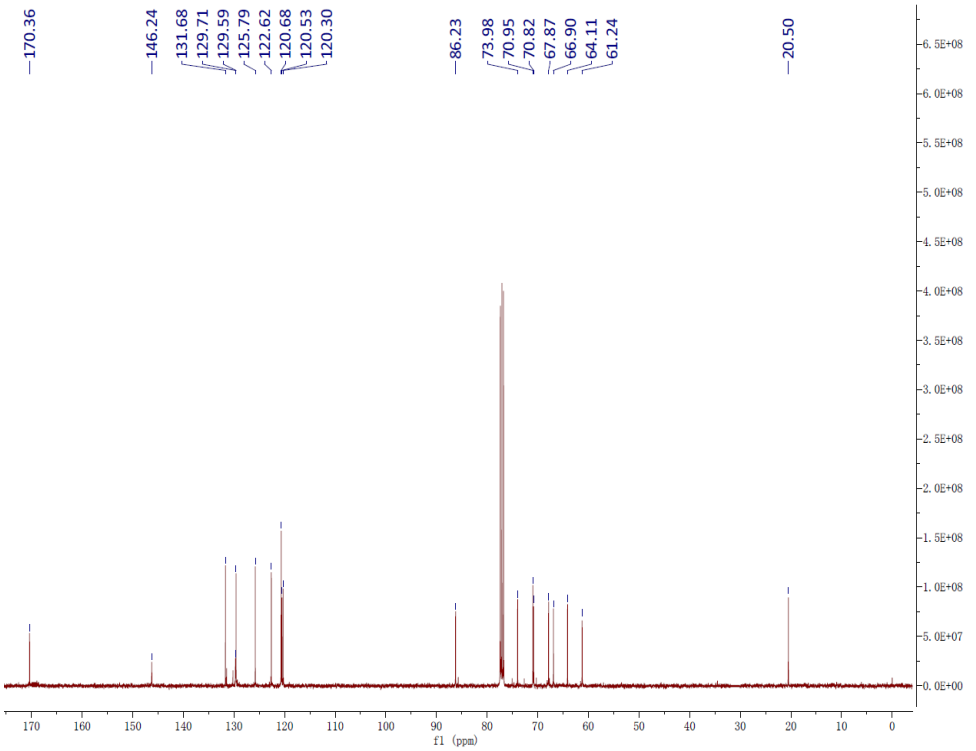

^{13}C NMR of **PEG-pyr**.

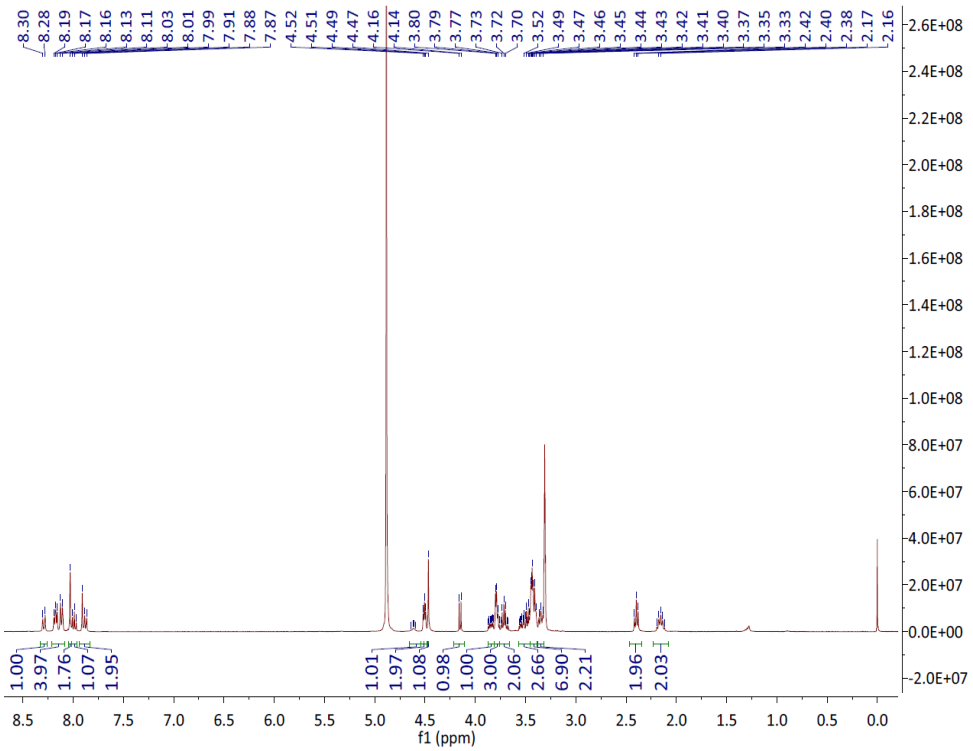

^{1}H NMR of **Gal-pyr**.

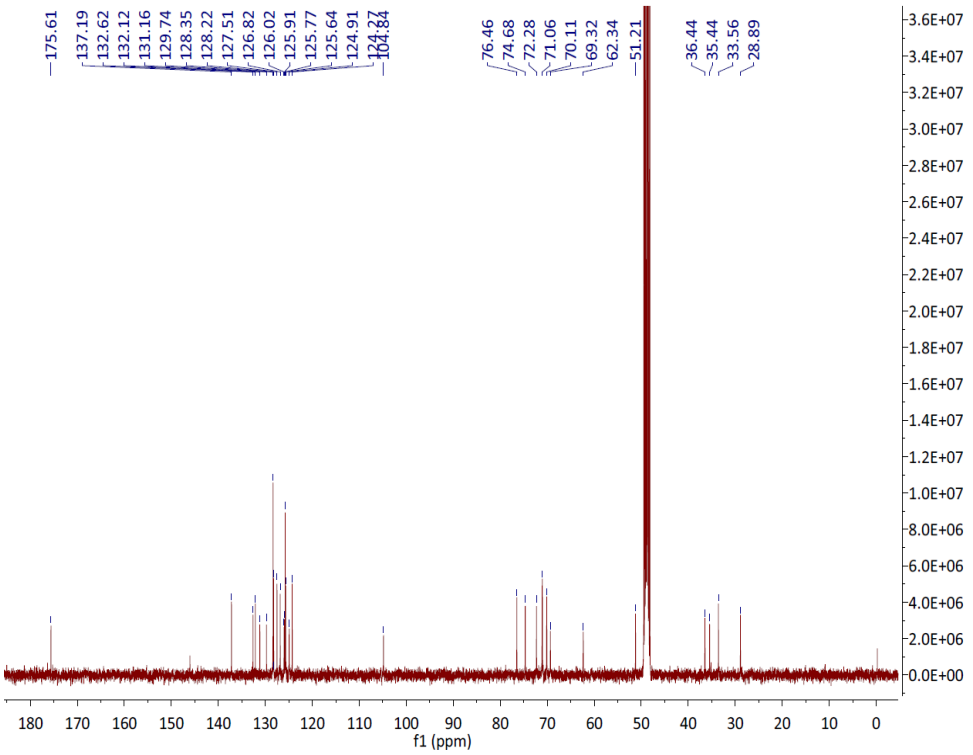

^{13}C NMR of **Gal-pyr**.

4 Additional References

1 K.-B. Li, N. Li, Y. Zang, G.-R. Chen, J. Li and T. D. James, *Chem. Sci*., 2016, **7**, 6325-6329.

2 C. Ahlborn, K. Siegmund and C. Richert, *J. Am. Chem. Soc*., 2007, **129**, 15218-15232.

3 Y.-J. Huang, W.-T. Dou, F.-G. Xu, H.-B. Ru, Q.-Y. Gong and D.-Q. Wu, *Angew. Chem. Int. Ed*., 2018, **57**, 3366-3371.

4 S. M. Chowdhury, C. Surhland, Z. Sanchez, P. Chaudhary, M. A. Suresh Kumar, S. Lee, L. A. Pena, M. Waring, B. Sitharaman and M. Naidu, *Nanomedicine*, 2015, **11**, 109-118.

5 R. K. Mishra, E. Segal, A. Lipovsky, M. Natan, E. Banin and A. Gedanken, *ACS Appl. Mater. Interfaces*, 2015, **7**, 7324-7333.

6 X. Wang, O. Ramstrom and M. Yan, *J. Mater. Chem*., 2009, **19**, 8944-8949.

7 M. Mathias, D. -F. Stefano, R. Ute and H. Susanne, *Nat. Protoc*., 2010, **5**, 1460-1469.

8 K. Hatano, H. Saeki, H. Saeki, H. Aizawa, T. Koyama and K. Koyama, *Tetrahedron Lett.*, 2009, **50**, 5816-5819.

9 A. M. Alanazi and A. S. Abdelhameed, *PLoS One*, 2016, **11**, e0146297.

10 K. R. Wang, H. W. An, D. Han, F. Qian and X. L. Li, *Chinese Chem. Lett.*, 2013, **24**, 467-470.

11 O. Srinivas, N. Mitra, A. Surolia and N. Jayaraman, *J. Am. Chem. Soc*., 2002, **124**, 2124-2125.

12 A. J. Cagnoni, J. Kovensky and M. L. Uhrig, *J. Org. Chem*., 2014, **79**, 6456-6467.

13 I. Otsuka, T. Hongo, H. Nakade, A. Narumi, R. Sakai and T. Satoh, *Macromolecules*, 2007, **40**, 8930-8937.

14 K. J. Neurohr, N. M. Young and H. H. Mantsch, *J. Biol. Chem.*, 1980, **255**, 9205-9209.

15 C. M. Zhao, K. R. Wang, C. Wang, X. He and X. L. Li, *ACS Macro Lett*., 2019, **8**, 381-386.

16 Q. A. Besford, M. Wojnilowicz, T. Suma, N. Bertleff-Zieschang, F. Caruso and F. Cavalieri, *ACS Appl. Mater. Interfaces*., 2017, **9**, 16869-16879.

17 J. K. Ajish, A. B. Kanagare, K. S. A. Kumar, M. Subramanian, A. D. Ballal and M. Kumar, *ACS Appl. Nano Mater*., 2020, **3**, 1307-1317.

18 K. J. Neurohr, N. M. Young, I. C. P. Smith and H. H. Mantsch, *Biochemistry*, 1981, **20**, 3499-3504.

19 K. J. Neurohr, N. Mantsch, M. Young and D. R. Bundle, *Biochemistry*, 1982, **21**, 498-503.

20 K. Kim, K. Matsuura and N. Kimizuka, *Bioorgan. Med. Chem.*, 2007, **15**, 4311-4317.

21 A. Vargas-Berenguel, F. Ortega-Caballero, F. Santoyo-González, J. J. García-López, J. J. Giménez-Martínez and L. García-Fuentes, *Chem. Eur. J.*, 2002, **8**, 812-827.

22 X. Zhang, F. Pastorino and G. Simone, *Sensor. Actuat. B-Chem*., 2018, **273**, 342-349.

23 X. Wang, E. Matei, A. M. Gronenborn, O. Ramström and M. D. Yan, *Anal. Chem*., 2012, **84**, 4248-4252.

24 P. M. Rendle, A. Seger, J. Rodrigues, N. J. Oldham, R. R. Bott and J. B. Jones, *J. Am. Chem. Soc*., 2004, **126**, 4750-4751.

5 Author contributions

Y. S., S. Z., H.-Q G. and F. X. carried out synthesis and supramolecular assembly under the supervision of X.-P. H., Y. M. and L. Z. Y. S., S. Z. and H.-Q. G. carried out characterization of materials under the supervision of X.-L. H. and Y. M. H.-Q. G. and K.-C. Y. carried out microbiological studies under the supervision of D. C. X.-L. H. wrote the manuscript with the support of X.-P. H., T. D. J., Y. M., F. X., L. Z. and D. C. X.-P. H., Y. M., L. Z., X.-L. H. and D. C. obtained funding for the research. All authors read and approved the final manuscript.